SUPPLEMENT TO THE *WELDING JOURNAL,* AUGUST 2014
Sponsored by the American Welding Society and the Welding Research Council

Flux-Coating Development for SMAW Consumable Electrode of High-Nickel Alloys

Extrudability, recovery analysis, and welding characteristics were incorporated into a shielded metal arc welding electrode for welding high-nickel alloys

BY K. SHAM AND S. LIU

ABSTRACT

There is interest in improved high-nickel alloy electrodes for shielded metal arc welding (SMAW) to replace gas tungsten arc welding (GTAW) with cold wire feed for pressure vessel fabrication/repair in the power-generation industry. Without altering the GTAW wire composition, a proper flux coating was designed to produce a SMAW electrode to give an enhanced weld composition. SMAW electrodes were designed by developing proper flux coatings for extrusion, welding characteristics, and weld integrity. The flux formulation design began with an equal distribution of three primary ingredients: cryolite, rutile, and calcium carbonate to clean the weld, create a slag, and provide shielding gas, respectively. The system was then optimized to enhance extrudability, slag detachability, electrode weldability, alloying recovery, arc stability, and a number of weld properties. Detailed mass balance calculations were performed to determine alloying element transfer across the arc and to understand weld metal recovery from the flux coating, filler metal wire, and base metal. For chromium and manganese, an average of 95 and 60% weld recovery was confirmed and determined, respectively. The elemental recovery data determined were important for calculating the proper additions of these elements into the flux formulation. Comparisons revealed comparable welding characteristics for the in-house manufactured and commercial SMAW electrodes. Arc voltage analysis was also performed to determine arc stability of these electrodes. Results indicated differences in metal transfer modes between the different flux coating iterations, and the final electrodes exhibited more consistent voltage-time traces. This work demonstrates that even though it is common practice to use a GTAW wire to build a SMAW electrode, the flux coating can be designed to beneficially alter the weld composition.

KEYWORDS

•Covered Electrode • SMAW Consumable • Nickel Alloys • Flux Coating
•Extrusion • Electrode Manufacture • Composition

Introduction

With the development of a weld composition that demonstrates abilities to mitigate ductility dip cracking (DDC) and hot cracking in high-nickel alloys while maintaining their high temperature and corrosion resistance, an existing GTAW wire was used as an SMAW core rod with a flux coating designed specifically to meet the new predefined target weld metal composition. This work presents a design methodology for developing a flux coating formulation to convert a GTAW wire into a SMAW consumable electrode for high-nickel alloys.

The primary functions of the flux coating of an SMAW consumable electrode are to provide arc stability, protect the molten metal from the atmosphere, and refine the weld pool (Refs. 1, 2). Other functions of a flux coating include providing a slag layer for a smoother weld contour and bead shape, and surface cleanliness of the weld metal. Additionally, the flux coating should be formulated with ingredients that produce a low-density slag, provide proper viscosity for out-of-position welding, promote slag detachability, and reduce spatter and fume.

Fluxes can be separated into acidic, basic, and neutral depending on which oxides are dominant as flux ingredients. The combination of these oxides determines the slag properties such as melting temperature, thermal expansion, density, electrical conductivity, and viscosity. Acidic oxides such as silicates are primarily slag or network formers. Basic oxides (CaO, MgO, Na_2O and K_2O) decrease viscosity since they break down silica networks. Fluorides and chlorides are also added to selected flux compositions as aggressive chemicals that assist in removing strong oxides from the weld joints. Additions of fluorides decrease the viscosity of the slag, depending on the type of fluoride. Slipping agents and binding agents are added to improve the flow of the wet flux mixture during extrusion and bind the flux ingredients to each other and to the core rod to form a solid coating. Sodium silicate, potassium silicate, or mixtures of the two are common binders used to manufacture electrodes.

Welding arc stability is important to the weldability of the electrode and the integrity of the weld properties. Some ingredients used to enhance arc stability are potassium silicate, sodium silicate, rutile (TiO_2), and potassium

K. SHAM and S. LIU are with Colorado School of Mines Golden, Colo.

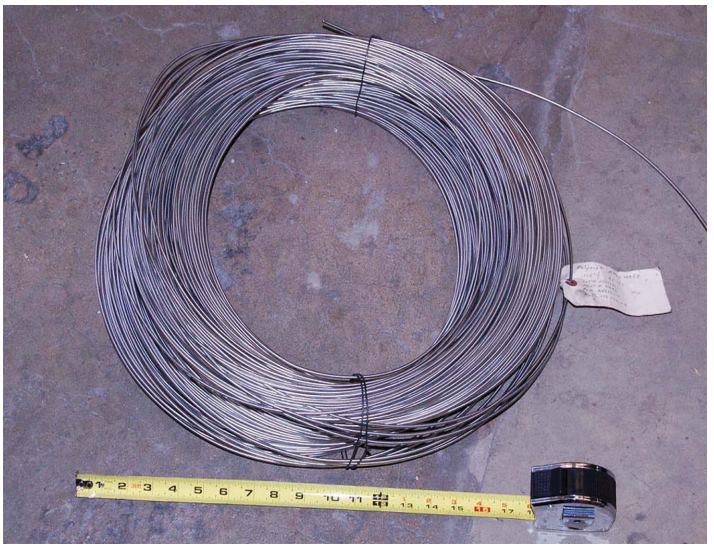

Fig. 1 — Experimental GTAW wire in coil form.

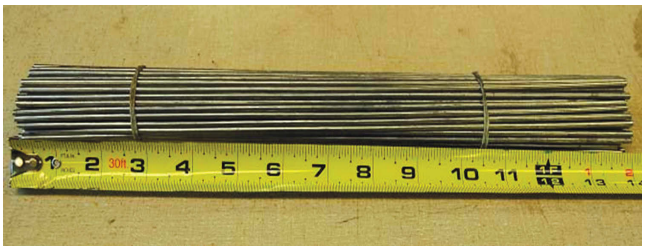

Fig. 2 — Experimental GTAW wire de-coiled, straightened, and cut into 356-mm (14-in.) lengths.

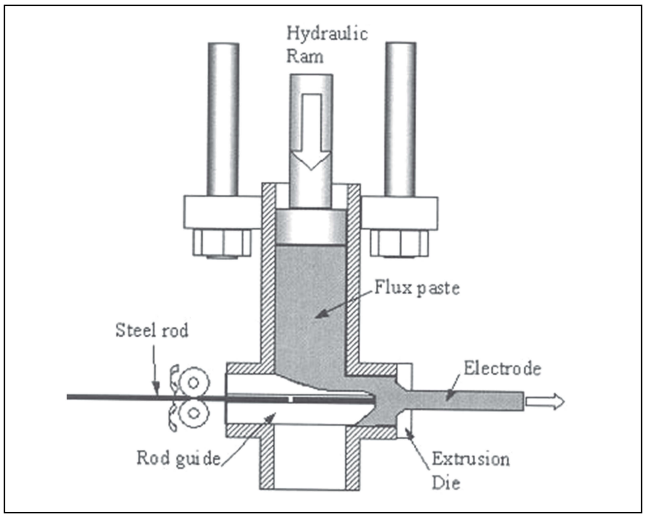

Fig. 3 — Schematic illustration of the extruder, top view (Ref. 14).

Table 1 — Commercial High-Nickel Core Rod Compositions

Element	E-1 (wt-%)	E-2 (wt-%)
Carbon	0.006	0.028
Silicon	0.05	0.16
Chromium	16.8	27.3
Manganese	2.5	0.37
Niobium	0.06	0.02
Iron	8.75	10
Nickel	71.3	60.4

titanate (Ref. 3). Even though potassium silicate acts predominately as the binder in the flux coating, it plays a critical role in the stabilization of the arc in AC applications because potassium ionizes at a lower energy, 4.3 eV/atom. Sodium ionizes at 5.1 eV/atom and is therefore more readily used as the binder for arc stabilizer of DC applications where the ability to reestablish the welding arc is not as vital (Ref. 4). The addition of fluorides typically produces a more erratic arc, despite its ability to remove surface oxides from the joint region.

Slag detachability is of great concern because the presence of slag on the weld surface will influence the integrity of multipass weldments and affect process economics. Rutile-containing fluxes generally produce slags that exhibit good detachability. On the other hand, basic flux systems typically exhibit less than desirable wetting. Consequently, complete slag removal may be more difficult in these systems. Slag removal has also been documented as more difficult when the flux coating contains fluorides. Slags that contain the spinel ($AO.B_2O_3$) where A and B represent cations such as Mg and Al and cordierite ($Mg_2Al_4Si_5O_{18}$) glass structure have also been deemed difficult to detach from the weld metal. An increase in alumina content in the flux composition has shown improved slag detachability. Another important factor to consider for slag detachability is the difference in coefficient of thermal expansion (CTE) between the slag and the weld metal deposit (Refs. 5–7). It is desirable to have a slag with a CTE different from that of the weld metal. Too early slag detachment, however, may present undesired heavy temper colors (Ref. 1). To further explain the thermal expansion mismatch, Equation 1 describes the strain that is produced due to a temperature change at the bonding interface between the slag and the weld metal.

$$S = \Delta\alpha(\Delta T) \quad (1)$$

S is defined as the strain, the $\Delta\alpha$ is the difference between the thermal expansion of the slag and the weld metal, and ΔT, known as the differential contraction, is defined as the temperature difference at the bonding interface during the welding thermal cycle (Ref. 8).

Another important aspect of the flux coating of the SMAW consumable electrode is that it can be utilized as a conduit for alloying the weld metal composition. The flux coating ratio defined as the diameter of the core rod divided by the diameter of the SMAW electrode affects the amount of alloying elements recovered in the weld metal (Refs. 9–11). There are three main components that contribute to the end weld composition: the core rod, the base metal, and the flux coating. Thus, it is important to obtain chemical compositions for all three components in order to calculate recovery directly from the flux coating.

Delta quantity is described as the amount of a specific element that is gained or lost during the welding process. The delta quantity is represented by the following mathematical equation:

$$(\Delta\text{Quantity})_i = (\text{Analytical Content})_i - (\text{Estimated Content})_i \quad (2)$$

The analytical content of element *i* is determined by chemical analysis of the

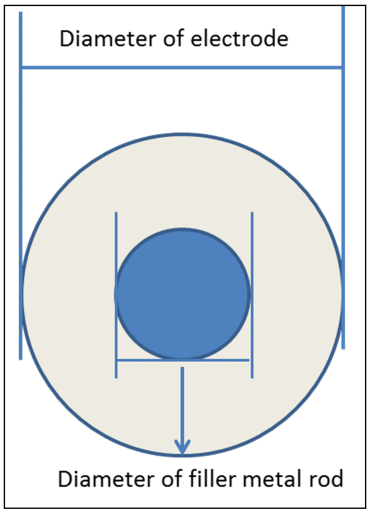

Fig. 4 — Pictorial depiction of diameter of filler metal rod and diameter of electrode.

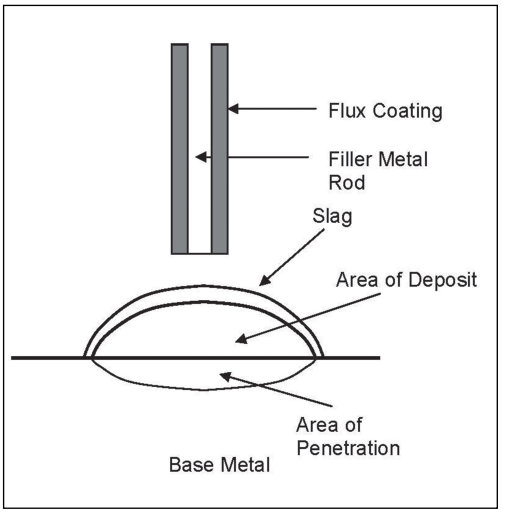

Fig. 5 — Schematic of SMAW.

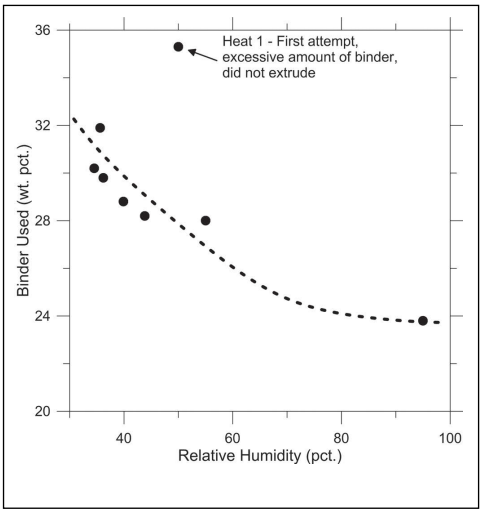

Fig. 6 — A relationship between the correct amount of binder added and the percentage of relative humidity in the working area.

weld metal, whereas the estimated content is determined by adding the contributions from the core rod and base metal. A negative delta quantity gives a loss of the specific element either to the slag or in a gaseous form. A positive delta quantity implies flux contribution of a specific element, having been transferred to the weld metal to achieve a certain target weld composition (Refs. 12, 13). The delta quantity concept plays an important part in understanding the role of the flux ingredients in their contribution to the final weld composition.

Experimental Procedures

Flux coating chemistries for commercial consumables were determined using a variety of techniques. The following techniques were all used together: X-ray diffraction (XRD), energy dispersive X-ray spectroscopy (EDS), wavelength-dispersive X-ray spectroscopy (WDS), atomic absorption (AA), and inductively coupled plasma optimal emission spectroscopy (ICP-OES). The combination of chemical analysis techniques are used together to determine both elemental composition and crystalline phases to determine possible mineral ingredients used to formulate the flux coatings.

Experimental wire of 3.2-mm (⅛-in.) diameter was procured in the form of a large coil (Fig. 1) that had to be decoiled, straightened, and cut into 356-mm (14-in.) lengths — Fig. 2. Table 1 gives the core rod compositions of the commercial SMAW electrodes ENiCrFe-3 (E-1) and ENiCrFe-7 (E-2) used for comparison in this research. Due to the sensitive nature of this work, the exact composition of the experimental wire is not revealed.

The experimental flux matrix presented in Table 2 displays all the major heats and changes to reach a final flux composition titled, "CSM Final." An initial formulation of a 1:1:1 mass ratio of cryolite (Na_2AlF_6), rutile, and calcium carbonate ($CaCO_3$) was taken as a starting point in the formulation process. The descriptors "decrease" and "increase" represent decreasing or increasing quantities of an ingredient from the previous heat to promote noticeable variations, in particular, slag properties or weld behavior. The matrix was designed to address the following properties: extrudability, flux coating finish, slag viscosity, slag de-

Table 2 — Experimental Flux Matrix for CSM High-Nickel SMAW Electrode Development

Flux Ingredient	Heat 1 (wt-%)	Heat 1A	Heat 2	Heat 3	Heat 4	Heat 5	Heat 6	CSM Final
Cryolite	21.6	Decrease	Increase	Decrease	Increase	Increase	–	–
Rutile	21.6	Decrease	Increase	–	–	–	–	Increase
Calcium Carbonate	21.6	Increase	Decrease	–	–	–	–	–
Silicon Dioxide	n/a	–	–	–	–	Increase	–	–
Talc	n/a	–	Increase	–	Decrease	Decrease	–	–
Kaolin Clay	n/a	Increase	–	Increase	–	Dercrease	–	–
Bentonite Clay	n/a	–	–	–	–	–	Increase	Decrease
Cellulose	n/a	–	–	–	–	–	–	Increase
Alginate	n/a	–	–	–	–	–	–	Increase
Ferroniobium	n/a	–	–	–	–	–	Increase	–
Manganese	n/a	–	–	–	–	–	Increase	–
Chromium	n/a	–	–	–	–	–	Increase	–
Binder	Bal.	Bal.	Bal.	Bal.	Bal.	Bal.	Bal.	Bal.

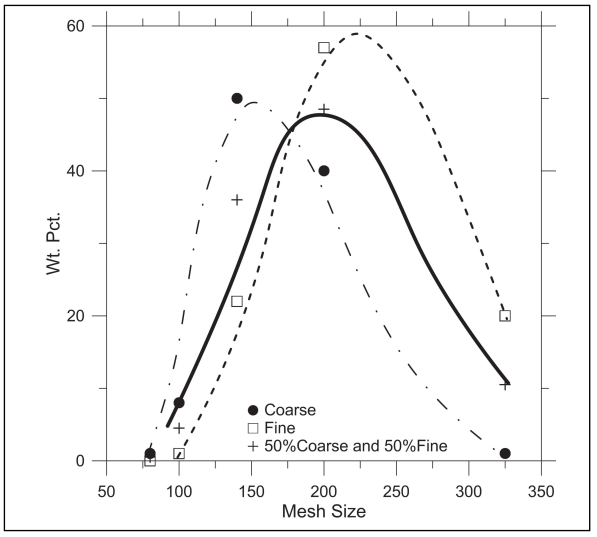

Fig. 7 — Particle size distribution for coarse, fine, and 50% coarse and 50% fine combined for rutile.

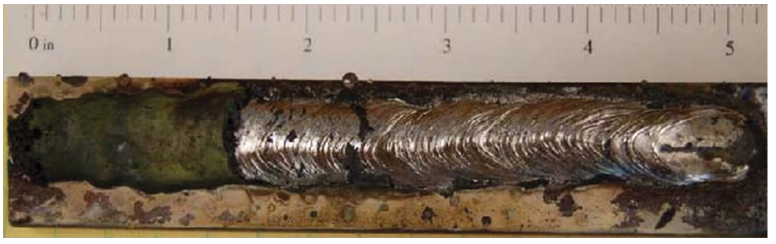

Fig. 8 — Bead-on-plate weld produced with Heat 2 flux composition. Part of the slag was retained for illustration.

Fig. 9 — Bead-on-plate weld produced with Heat 3 flux formulation with decreased cryolite content.

Table 3 — Welding Parameters for E-1, E-2, and CSM Final

Electrode	E-1	E-2	CSM Final
Electrode Feed Rate (mm/s)	4.9	4.9	5.1
Travel Speed (mm/s)	2.1	2.1	1.7
Deposition Rate (g/s)	0.57	0.62	0.45
Welding Time (s)	36	43	42

tachability, effect of cryolite on weld cleanliness, welding characteristics, arc stability, alloying additions, and SMAW electrode mass production.

Manufacturing SMAW Consumable Electrodes

For the SMAW consumable electrode extruder, a total of 2 to 3 kg (approximately 4 to 6 lb) of the wet mix is needed to make a successful extrusion run. The extruder used for the experimental small batch production for this work is capable of pressures ranging from 500 to 1000 lb/in.^{2} (3.5 to 6.9 MPa) as compared to a commercial extruder averaging around 5000 to 6000 lb/in.^{2} (35 to 40 MPa). Figure 3 gives a detailed top-view schematic of how the extruder functions during extrusion. A successful extrusion is dependent on many factors such as experience with the extruder, successful adjustment of the eccentricity of the electrodes, proper preparation of the core rods, adding the right amount of binder and slipping agent, adequate flux coating ratio, and having a good particle size distribution for the dry mix. One major manufacturing aspect of concern is electrode eccentricity, which affects the weldability of the SMAW consumable electrode. Electrode eccentricity is measured by the relative position of the core rod with respect to the layer of flux coating. An eccentric electrode with uneven thickness coating surrounding the core rod will produce an erratic arc with uneven melting of the core rod and preferential flaking of the flux coating.

Another important aspect of extrusion is determining the appropriate thickness of the flux coating, which is adjustable during manufacturing. Inappropriate flux coating thickness can affect the integrity of the weld and the composition of the weld metal. The thickness of the flux coating is measured as a flux coating ratio defined as the ratio between the electrode diameter and the diameter of the core rod — Fig. 4. Commercial electrodes showed an average flux coating ratio of 0.4. Thus, a die size comparable to 0.4 was used for the manufacturing of the in-house manufactured electrodes giving an average flux coating ratio of 0.42. Calipers and image analysis were used to verify results. After drying in air for 24 h following extrusion, the electrodes were then baked in an oven at 175°C (350°F) for one h, 260°C (500°F) for three h, and then 175°C (350°F) for one h. The drying sequence was consistent with industrial practice and selected after input from commercial electrode manufacturers (Ref. 11).

Welding Process

Using ASTM A36 base plates and Inconel® 690 base plates for the final welds, bead-on-plate welds were deposited using a Hobart TIG-300 constant current power supply. Using direct current electrode positive (DCEP) configuration, an average linear heat input of 12 kJ/mm (0.5 kJ/in.) was obtained. Based on the manufacturer-recommended welding ranges for E-1 (90–110 A) and E-2 (75–100 A), the respective averages of 100 A and 88 A were adopted for welding for the 3.2-mm- (⅛-in.-) diameter commercial electrodes. The optimal welding current for the in-house manufactured electrode was subsequently determined to be 85 to 95 A. Table 3 gives the welding parameters for E-1, E-2, and the "CSM Final." Arc signals were acquired during the welding process for the bead-on-plate samples for both the commercial and in-house manufactured electrodes. These voltage signals were obtained using a data

Fig. 10 — Bead-on-plate produced with CSM Final flux formulation with cryolite adjusted to 24 wt-%.

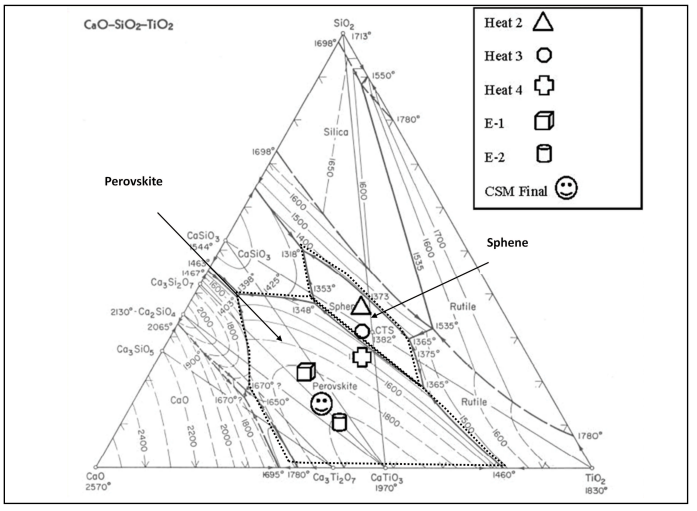

Fig. 11 — Ternary phase diagram of CaO-TiO_2-SiO_2 (Ref. 15) with compositions marked.

acquisition system with a sampling rate of 1000 Hz and LabView® 7.1. These digital voltage signals were recorded for the duration of every weld, which ranged from 35 to 50 s.

$$AFMC(G)=\left(1-\left(\frac{RE(in)}{IE(in)}\right)\right)\times AFM(g) \quad (3)$$

Chemical Compositions and Recovery Calculations

The chemical compositions of the base metal, all the filler metal wires, and welds were analyzed using OES. Filler metal wires were also melted into buttons to simulate the chemical recovery of arc welding in an inert atmosphere. Alloying element recovery calculations were done with the measured compositions. Dilution calculations were performed on all bead-on-plate welds in order to calculate alloying element recovery in the weld metal. Dilution percentage of a bead-on-plate weld was calculated as 37.1%. With these known contributions from the base metal and the filler metal, the weld composition can be determined numerically. Weld metal recovery was determined for each of the major alloying elements: niobium, manganese, and chromium.

A mass balance calculation was conducted to determine the actual amounts of the electrode consumed (both weight and length) to form the weld. The amount of weld deposit (area of deposit and area of penetration) was also determined using *ImageJ*® for the mass balance calculations. *ImageJ* is a public domain image processing software developed at NIH (National Institute of Health). With all the data necessary, a series of calculations using the equations below was performed in sequence. Figure 5 displays all aspects of SMAW to assist in the understanding of the recovery calculations that follow.

$$FM(g)=AFMC(g)\times\left(\frac{OES-FM(wt\%)}{100}\right) \quad (4)$$

$$AFCC(g)=\left(1-\left(\frac{RFC(in)}{IFC(in)}\right)\right)\times AFC(g) \quad (5)$$

$$FC(g)=AFCC(g)\times\left(\frac{FC(wt\%)}{100}\right) \quad (6)$$

$$BMP(g)=AP(cm^2)\times LW(cm)\times\frac{7.8g}{cc} \quad (7)$$

$$BM(g)=BMP(g)\times\left(\frac{OES-BM(wt\%)}{100}\right) \quad (8)$$

$$WM(g)=(BMP(g)+WMD(g))\times\left(\frac{OES-WM(wt\%)}{100}\right) \quad (9)$$

After completing calculations using Equations 3–9 for each element of interest, the following Equation 10 is used to determine the actual overall weld recovery:

$$WMR_i=\left(\frac{Z_w}{Z_f+Z_r+Z_{bm}}\right)_i\times 100\% \quad (10)$$

where *WMR* is weld metal recovery, *Z* represents the concentration of the element *(i)* in discussion, *w* is the weld metal, *f* is the flux coating, *r* is the filler metal core rod, and *bm* is the base metal.

Results and Discussion

The flux coatings of the two commercial nickel-alloy electrodes, E-1 and E-2, were examined as references for comparison with the flux formulation effort in this investigation. Table 4 presents the compositions of the E-1 and E-2 flux coatings. As can be seen, the three principal ingredients in the flux coating of commercial high-nickel SMAW electrodes are cryolite, rutile, and calcite. E-1 contained a fourth major ingredient, feldspar, which is generally treated as filler material, added mainly for slag volume. A combination of strontium and calcium carbonate was used in the commercial flux coatings because strontium carbonate decomposes at a higher temperature, 1100°C (2012°F), than calcium carbonate and provides better coverage to the weld pool. An additional advantage of strontium carbonate is that it is not as hygroscopic as calcium carbonate. Picking up less moisture, the electrode flux coating is expected to produce a more stable arc. The E-2 flux coating contained a small amount of silica and some other alloy-

Fig. 12 — Self releasing slag systems, E-1 (top) and CSM Final (bottom).

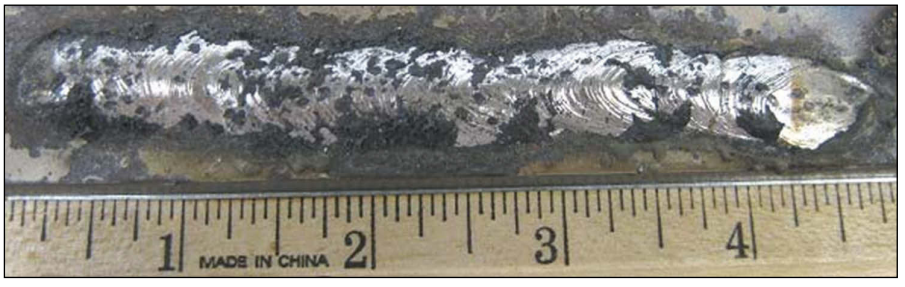

Fig. 13 — Heat 2 bead-on-plate exhibiting poor slag detachability.

ing elements for weld composition adjustment such as manganese, nickel, and chromium. Due to the inert nature of nickel, the value and importance of a chemically aggressive flux ingredient cannot be overemphasized. Together with fluorides that are chemically aggressive for cleaning the weld joint, cryolite prevents joint surfaces from oxidation and improves the cleanliness of the weld metal surface. Rutile primarily functions as a slag former and arc stabilizer. Calcium carbonate decomposes around 890°C (1634°F) into CaO and CO_2. CaO serves as a slag former by reacting with TiO_2 and SiO_2. CO_2 is the shielding gas that displaces the air from the weld joint and blankets the entire weld region. The performance of each flux formulation determined the amounts of addition or subtraction of each of the ingredients for the subsequent formulation.

Evaluation of Electrode Extrudability

Extrusion of SMAW electrodes is not a process that can be easily quantified. It depends on a number of variables including the type and source of the mineral, the appropriate amount of water, the particle size distribution, among others. The extrusion variables studied were the amount of binder, the mixing technique, the slipping agents, and the particle size distribution of the dry mix. The extrusion environment is also critical. For example, relative humidity and temperature affect significantly the flow characteristics of the wet mix during extrusion. An extrudable flux can quickly lose moisture and become difficult to extrude during the time of manufacturing one batch of electrodes. Therefore, this process is subjective and based on experience in observing the consistency of the wet mix, the fluidity of the wet mix, and the adhesion between the core rod and the flux coating.

Extrusion was performed on each of the experimental flux formulations, including the base formula, to verify the extrudability of the flux mixtures. As expected, the first flux formulation, Heat 1, was not extrudable because an excessive amount of the binder (at ~35 wt-%) was utilized. Since the binder is typically 50% silicate and 50% water, some data were collected to determine if the amount of binder added is dependent on the humidity of the manufacturing environment. The correct amount of binder is dependent on the relative humidity of the working area at the time of mixing and extrusion. The relative humidity in the laboratory fluctuated

Table 4 — E-1 and E-2 Flux Coating Composition

Mineral	E-1 (wt-%)	E-2 (wt-%)
Cryolite (Na_3AlF_6)	21	25
Rutile (TiO_2)	14	17
Strontium Carbonate ($SrCO_3$) and Calcium Carbonate ($CaCO_3$)	24	28
Silicon Dioxide (SiO_2)	n/a	7
Feldspar ($K_2O.Al_2O_3.6SiO_2$)	23	n/a
Manganese	13	12
Nickel	1	2
Iron	n/a	3
Chromium	n/a	3

between 34 and 55% with an average relative humidity at 42%. The average amount of binder added to the dry mix to form the wet mix was 30 wt-% with a standard deviation of less than or equal to 2.5 wt-% depending on the humidity. When the relative humidity was above the average relative humidity of 42%, the amount of binder was less than 30 wt-% but within the deviation of 2.5 wt-%. Figure 6 gives a graphical representation of the relationship between binder amount and relative humidity in the working area. The point with the highest relative humidity of 95% was data recorded during the mass production of the electrodes at a commercial electrode manufacturer in Houston, Tex. It can be seen that the amount of binder needed in making the wet mix decreases as the relative humidity of the work area increases with 23.5 wt-% of binder being the lowest amount of binder needed.

The poor extrudability of Heat 1 led to a decrease in binder and the addition of a slipping agent, kaolin [$Al_2Si_2O_5(OH)_4$], to the flux paste to improve electrode extrusion. Heat 1A had improved extrudability with too much slipping agent added; the flux paste flowed faster than the rod intermittently even though the velocity of the compressor was decreased to a minimum. For Heat 2, a combination of kaolin and talc, $Mg_3Si_4O_{10}(OH)_2$, was used in a decreased amount from Heat 1A. These two slipping agents greatly improved extrudability of the base flux coating. For the latter extrusion runs of the nickel SMAW consumable electrodes, including the larger batches, bentonite clay, [$Al_2O_3(4SiO_2H_2O)$] was used instead

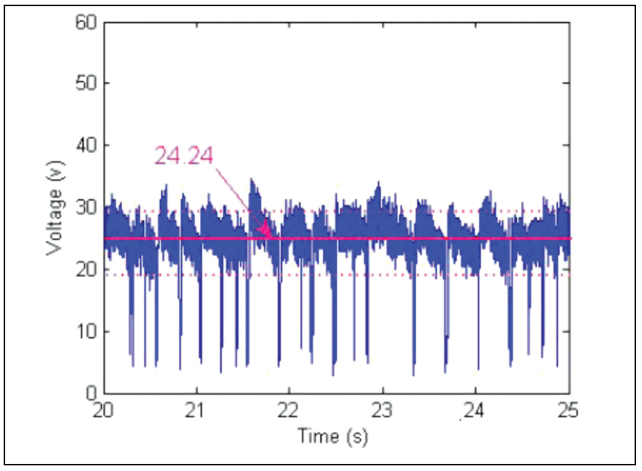

Fig. 14 — Voltage data for E-1.

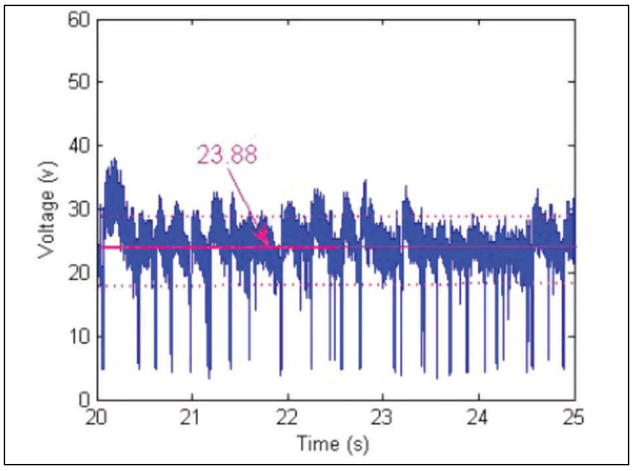

Fig. 15 — Voltage data for E-2.

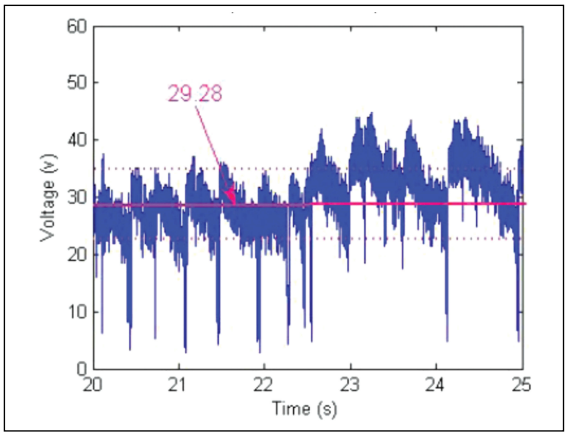

Fig. 16 — Voltage data for Heat 2.

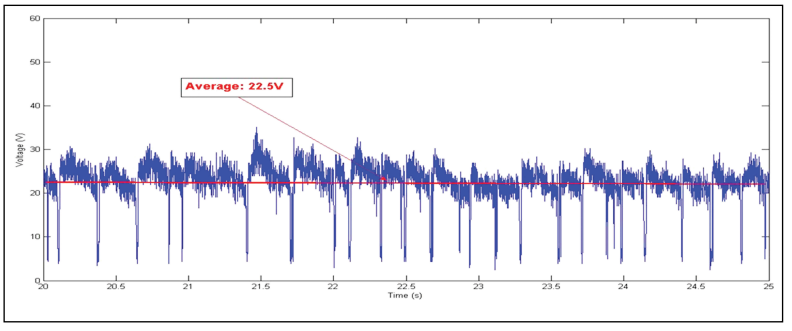

Fig. 17 — Voltage data for CSM Final.

of kaolin clay due to what was available. Other than the difference in chemical composition, both bentonite clay and kaolin clay, and talc function as slipping agents to ease extrudability. Availability, proper particle size distribution, and desired weld composition may be the deciding factors for selecting one and not the others. Finally, a small quantity of cellulose was added to enhance homogeneous mixing of the wet mix during the commercial mass production. To maintain extrudability and minimize water absorption, a small amount of alginate was added as a slipping agent.

In Heat 5, the amount of slipping agent was further reduced and a better particle size distribution for the dry mix was used to maintain extrudability. In addition to the extrusion aspect, particle size distribution of the dry mix also affects the flux coating finish of a SMAW electrode. Using the combination of slipping agents, proper mixing technique, the correct amount of binder, and an improved particle size distribution, "CSM Final" gave a much improved extrusion experience. The dry mix of the CSM Final was optimized by using 50 wt-% fine grades and 50 wt-% coarse grades for the calcium carbonate and rutile. Figure 7 depicts an example of how the combination of the fine and coarse grades of rutile affected the overall particle distribution. As compared to Heat 1, which consisted of larger quantities of 325 and 400 mesh size, "CSM Final" had lesser quantities of 325 and 400 mesh size and displayed a more normal distribution around 200 mesh, which is the practice of industry formulators. The CSM Final electrodes have good extrudability and their flux coatings have a smooth appearance.

Weld Cleanliness

The first experimental Heat 1 of the flux formulation used an even distribution of cryolite, rutile, and calcium carbonate as the starting point. Heat 1A and Heat 2 contained 18–19 wt-% of cryolite, which produced weldments with good surface cleanliness. Surface cleanliness was inspected visually with a shiny, silvery weld having good surface cleanliness. Figure 8 depicts a bead-on-plate weld produced with Heat 2 from the experimental flux coating design matrix displaying good surface cleanliness. To test the effectiveness and optimal amount of cryolite as a chemically aggressive flux ingredient to enhance the cleanliness of the weld metal, the amount of cryolite was decreased from 19 wt-% in Heat 2 to 13 wt-% in Heat 3. As a result, the bead-on-plate weld from

Table 5 — Flux Ingredients Broken Down into the Slag Form

Flux Ingredients		Primary Oxides in Slags
Na_3AlF_6		Na_20, Al_2O_3
TiO_2		TiO_2
$CaCO_3$		CaO
$Al_2Si_2O_5(OH)_4$	⇒	Al_2O_3, SiO_2
$Mg_3Si_4O_{10}(OH)_2$		MgO, SiO_2
SiO_2		SiO_2
$K_2SiO_3.nH_2O$		K_2O, SiO_2

Table 6 — Room Temperature CTE Values of Two Glass Phases and Inconel 600 and 690 Alloy (Refs. 15–18)

Materials	CTE at RT (10^{-6}/°C)
Sphene ($CaTiSiO_5$)	6
Perovskite ($CaTiO_3$)	15.8
Inconel 690 alloy	10.4

Table 7 — Weld Recovery Results (wt-%)

Elements	Heat 2 (%) Alloy 1	Heat 2 (%) Alloy 2	E-2 (%)	E-1 (%)
Chromium	100	100	100	88
Manganese	54	65	47	51
Niobium	89	100	n/a*	n/a*
Iron	100x	100	94	95
Nickel	83	99	100	100

**Note — Niobium composition was not determined.*

Table 8 — Known Alloy Recovery from SMAW Flux Coating (wt-%) (Ref. 5)

Alloy Element	Form of Material in Electrode Covering	Approximate Recovery of Element, wt-%
Aluminum	Ferroaluminum	20
Boron	Ferroboron	2
Carbon	Graphite	75
Chromium	Ferrochromium	95
Niobium	Ferroniobium	70
Copper	Copper Metal	100
Manganese	Ferromanganese	75
Molybdenum	Ferromolybdenum	97
Nickel	Electrolytic nickel	100
Silicon	Ferrosilicon	45
Titanium	Ferrotitanium	5
Vanadium	Ferrovanadium	80

Heat 3 produced a dull, oxidized weld metal surface finish — Fig. 9. In Heat 4, cryolite was increased back to the 19 wt-% used in Heat 2 to restore weld cleanliness. In Heat 5, cryolite was further increased to optimize weld cleanliness. The "CSM Final" flux formulation optimized cryolite to 24 wt-% and the respective bead-on-plate weld can be seen in Fig. 10. The "CSM Final" bead-on-plate weld displays the lustrous, silvery metallic appearance of nickel that Heat 3 (Fig. 9) does not with the decreased amount of cryolite. Cryolite plays a critical role in the cleanliness of the weld metal surface. The amount must be optimized for weld cleanliness without affecting the viscosity of the slag flow since fluorides act as network breakers and decrease the viscosity of the slag. Part of the design methodology for flux coatings in a SMAW consumable electrode is to balance the multiple functions of each flux ingredient to optimize extrudability, weldability, and weld integrity.

Slag Detachability

Slag detachability is defined as the ease with which the solidified protective slag layer can be removed. Poor slag detachability can negatively impact productivity and weld integrity. The differences in the CTE between the slag and the weld metal play a vital role in the ability for the slag to detach easily.

Using a phase diagram of the CaO-TiO_2-SiO_2 ternary system, shown in Fig. 11, mass balance equations were used to estimate the glass phases produced in the slag. To perform these mass balance equations, the flux ingredients were first broken down to their respective slag form (expressed in the form of primary oxides)—Table 5). Similar oxides were then grouped together such that the ternary system diagram of CaO-TiO_2-SiO_2 can be used. Na_2O, MgO, and K_2O were grouped together with CaO, and Al_2O_3 was grouped with TiO_2. This approximation does not give an exact composition of the slag, but the methodology allows for the estimation of the predominant glass phase in the slag. The determination of the dominant glass phase allows the estimation of the differences in the CTE values between the slag and weld metal, which helps predict slag detachability. Values of linear CTEs were collected from literature for the weld metal and the various crystalline phases that could be formed based upon the composition of the flux coating. These values are shown in Table 6. With the compositions of the E-1 and E-2 flux coatings, calculations were made to determine the respective crystalline phases that could form in the resulting slags. As can be seen in Fig. 10, the two commercial slags were determined to produce the perovskite phase, which has a larger CTE, 15.8×10^{-6}/°C, than that of the weld metal, 10.4×10^{-6}/°C (Refs. 15, 18). The CTE of Inconel® 690 alloy is used for the weld metal since it is the most similar to the composition of the experimental weld wire used.

Figure 11 shows the ternary system with the respective phases that form for Heats 2 through "CSM Final," and the commercial electrodes. Examination of this figure shows that the commercial electrode compositions fell into the perovskite phase. Heat 2 produced a dominant sphere phase in the slag with a CTE of 6×10^{-6}/°C, which is smaller than the weld metal, 10.4×10^{-6}/°C, and displayed poor slag detachability. Heat 3 also produced a sphene phase with poor slag detachability (Ref. 15). Furthermore, the slag developed a porous layer that adhered tenaciously to the weld metal, which is an indication that a thin spinel phase is likely to be present on the surface of the weld bead. The occurrence of spinel on top of a weld bead is usually in the form of a thin layer on the order of several atomic layers thick. The thermal strain associated with contraction and expansion of this layer is typically small. As such, the spinel layer is expected to have great adhesion with the weld bead surface.

Heat 4 electrodes produced a dominant perovskite phase in the slag, which exhibited much better slag detachability due to the higher CTE values. With a CTE value that is higher than that of the weld metal of Inconel® 690 alloy, the perovskite

Table 9 — Recovery Results from the Button Melts with Respect to the Core Rods (wt-%)

Elements	Alloy 1 (wt-%)	Alloy 2 (wt-%)
Chromium	99	100
Manganese	95	89
Niobium	100	89
Iron	62	60
Nickel	100	100

Table 10 — Comparison of Core Rod and No-Dilution Weld Composition Compared to a Predefined Target Weld Composition (wt-%)

Elements	Target Weld Composition	Experimental Core Rod (HD 52)	Heat 5	Heat 6
Cr	27	26.8	24.7	27.2
Fe	2.5	2.6	2.91	4.9
C	0.035	0.012	0.009	0.02
Ti	0.3	0.15	0.03	0.05
Nb	2.5	1.82	1.11	2.58
Mn	3	3.02	2.12	2.97
Ni	Bal	Bal	Bal	Bal
S	<0.0015	0.001	0.001	<0.001
P	<0.005	0.001	0.001	0.005
Si	0.05	0.08	0.58	0.60
Mo	0.01	0.12	0.11	0.10
Cu	0.1	<0.1	0.0015	0.05

phase will contract much more than the weld metal upon solidification. The greater tensile stress induced in the slag phase will promote better slag detachability. In order to maintain slag detachability for CSM Final flux formulation, rutile was increased to enhance slag formation. The observations described above help to explain the slag detachability behavior observed in the experiments. CTE differences between the dominant slag phase and weld metal can be used as a tool to help design flux coatings with enhanced slag detachability.

Weld Metal Recovery

Following the series of calculations discussed in the experimental procedures section, Table 7 gives the weld recovery results of importance to the integrity of the weld metal. Chromium gives an experimentally determined average of 97% weld recovery with respect to the three sources of contribution, the core rod, the flux coating, and the base metal. Manganese displayed an average weld recovery of about 54%. This value was slightly lower than that typically used (around 70 to 80%) in the industry. However, being the major deoxidizer in the weld system, a low recovery rate is not entirely surprising. Niobium was only calculated for the in-house electrodes at an average recovery value of about 94%. The commercial electrodes were not taken into consideration because the niobium content in those fluxes was not determined. The ASM *Metals Handbook* Vol. 6 provided niobium recovery from the flux ingredient in the form of ferroniobium as 70% along with additional known alloy recovery from SMAW flux coating (Table 8) (Ref. 5). Another element of importance is the iron content, which must be carefully monitored because it too, like chromium, forms the undesirable $M_{23}C_6$-type carbide. Average measured values in this research gave iron recovery at 97%. Lastly, average recovery value of nickel was also calculated to be about 95%. These recovery values are important for the calculation of necessary additions in the flux coating for final weld composition.

Another series of recovery calculations was performed on the button melts to understand the percentage of recovery directly from the core rods without other influences. These results are shown in Table 9. Chromium and iron contents were almost 100% in recovery in an ideal welding atmosphere. The recovery of manganese from the commercial core rods (Alloy 1) averaged about 95% whereas the recovery of manganese from the in-house manufactured Heat 2 (Alloy 2) averaged about 89%. It is clear with this information that the replenishing of manganese must be made via flux. The ASM *Metals Handbook* reported recovery from ferromanganese flux as about 75%. Alloying through the flux must be done with the appropriate ingredients to minimize iron increase. Niobium recovery from the experimental core rods was relatively high at an average of 94%. Iron recovery from the core rods was reported as an average of 76%. The different recovery rates from the core rod and from the flux coating reported in this work are invaluable for future efforts in flux design and formulation.

The findings showed that it was possible to obtain reliable recovery values from all four of the most important alloying elements. These values were used to incorporate alloying additions in the flux coating design and optimization once the base flux formula was completed. The recovery rate used for chromium additions in the flux was 95%. A value of 60% was used for the manganese recovery in the flux coating. Since there were no calculated values of recovery percentages for niobium, the ASM *Metals Handbook* Vol. 6 value of 70% was taken as the recovery rate for alloy additions in the flux coating.

Using the recovery rates determined previously, mass balance calculations were performed to determine the amounts for replenishing the alloying elements. Two empirical values were used to predict the percentage of the alloying elements additions to achieve the target weld composition. Each electrode weighed an average of 20.5 g and the average weight of the flux coating was 10 g. These data originated from average calculations of weighed core rods and electrodes manufactured in-house at CSM. For chromium, a calculated 5% addition into the flux coating is required. For manganese and niobium, the calculated values were 3 and 4.1%, respectively. Using these calculated values, the target end weld composition was reached. These three main alloying additions were reached in each of the large batch extrusions demonstrating the robustness of the composition range. Note also that the last three extruded flux formulations possessed the same cryolite, calcium carbonate, rutile, ferroniobium, chromium, and manganese additions with small adjustments to other minor flux ingredients to obtain the correct amount of silicon and iron in the target weld composition.

The final base flux coating also served as the starting point for alloy-

Table 11 — Welding Observations at Optimal Welding Parameters

Electrode	E-1	E-2	Heat 2	Heat 3	Heat 4	CSM Final
Slag Detachability	Self Release	Good	Not Good to Poor	Not Good to Poor	Good	Self Release
Slag Thickness	Thinner, Porous	Thicker	Thicker	Thicker	Thicker	Thicker
Slag Flow	Less Viscous	Viscous	Viscous	Viscous	Viscous	Viscous
Arc	Soft, Stable	Harsh, Stable	Harsh, Less Stable	Unstable Arc	Unstable Arc	Soft, Stable

ing. Table 10 gives the chemical composition of the experimental high-nickel core rod (Alloy HD 52) used for manufacturing the SMAW consumable electrodes. Even though most of the elements are very close to the target weld composition (also defined in Table 10), alloying elements were lost through the SMAW process, thus requiring replenishment of chromium, niobium, and manganese as done in Heat 6. Using 95% recovery rate for chromium, 70% recovery rate for niobium, and 60% recovery rate for manganese, the compositions of these three elements were restored. Table 10 shows that the chromium, niobium, and manganese values in the no dilution weld composition paralleled those of the target weld composition.

The overall weight-percentage of rutile was increased approximately 5 wt-% to increase the oxygen content, which subsequently lowered the iron recovery without compromising niobium recovery. Silicon dioxide was removed to decrease the amount of silicon in the weld, but increasing the rutile content compensated for the removal of silicon dioxide to minimize silicon recovery since rutile is also a network former. Talc was also removed and one percentage of alginate was added instead as a better slipping agent without introducing more silicon into the flux system. The amount of bentonite clay was decreased a few pct. to lower the aluminum and silicon in the flux coating. For CSM Final formulation, the iron decreased from 4.9 to 3.6 wt-% and the silicon content was decreased from 0.6 to 0.1 wt-%. To achieve the predefined target composition of the no dilution weld metal, talc was completely removed and bentonite clay was decreased significantly.

Comparison of Qualitative and Quantitative Welding Characteristics

General qualitative and quantitative welding observations were documented for the characterization of the overall welding characteristics that each electrode displayed. Table 11 gives the qualitative characteristics for the commercial and in-house manufactured electrodes according to input from a group of professional welders. Comparing four experimental electrodes and two commercial electrodes, the best performing electrode was the CSM Final with a soft and stable arc, self-release slag, and thick, homogenous slag covering. Professional welders use the terms "harsh" and "soft" to describe their observation of the welding arc. A harsh arc generally implies a stronger arc force, but is more erratic in nature, and more difficult for a welder to control. A soft arc, on the other hand, is more uniform and easier for a welder to control. Feedback from several industrial welders confirmed these observations. Figure 12 shows the slags collected from E-1 and CSM Final to demonstrate good slag detachability. In contrast, slag detachability for Heat 2 was very poor as shown in Fig. 13, which shows the slag adhered tenaciously to the weld metal. All slag-related measurements were taken at a constant electrode melt rate. Slag thickness measurements were taken at various locations along the slag and consisted of the center and the side walls along the slag. The average thicknesses of E-1, E-2, and the CSM Final slag systems are given in Table 12. The commercial consumable designated E-1 had the thinnest average slag thickness at 1.52 mm. E-2 had an average slag thickness of 1.91 mm. The highest average slag thickness was the CSM Final at 2.03 mm.

Table 12 — Quantitative Values Related to the Slag

Electrode	Electrode Melt Rate ($mm*s^{-1}$)	Average Thickness (mm)
E-1	4.9	1.52
E-2	4.9	1.91
CSM Final	5.1	2.03

Arc Quality

The arc characteristics were described previously in a qualitative manner (Table 11). Arc voltage data were collected to characterize the arc stability and relate with the metal transfer modes during welding. During welding, E-1 and CSM Final both exhibited soft and stable arcs. E-2, however, displayed a harsh, bright, but stable arc. As to the intermediate flux systems, Heat 2 gave a less stable arc whereas Heats 3 (Fig. 9) and 4 gave unstable arcs due to electrode eccentricity issues. When an electrode is eccentric, the filler metal core rod is not centered in the flux coating causing the thinner side of the flux coating to burn away faster and the arc to blow out on that side. This causes the arc to widen and wander producing an unacceptable bead shape. Voltage signal analysis was not performed on Heat 3 and 4 because of the difficulties involved in welding with eccentric electrodes. The voltage data should assist in quantitatively substantiating the descriptive welding lingo of a harsh and soft arc.

Comparison of Welding Arc Signal Processing

The commercial electrodes, E-1 and E-2, exhibited lower average voltages of 24 and 23 V with a standard deviation of ±1.5 and ±2 V, respectively, and exhibited consistent and regular short-circuiting events — Figs. 14, 15. The in-house manufactured electrodes using Heat 2 displayed a higher average voltage of 29 V with a standard deviation of ±1.9 V. Heat 2 displayed mainly short-circuiting metal transfer mode with some globular events occurring in-be-

tween. Figure 16 shows a portion of the voltage data from Heat 2 displaying the change from short-circuiting to globular metal transfer mode. Changes in metal transfer modes throughout the welding of an electrode show problems with arc stability. Considering an electrode feed rate of 5.5 mm/s for Heat 2, these droplets were quite sizeable. Large globular transfer is generally an indication of transfer instability and spatter. CSM Final average voltage was 22.5 V with a standard deviation of ±1.6 V — Fig. 17. The dominant transfer mode for E-1, E-2, and CSM Final is short-circuiting occurring at similar frequencies. The frequencies of the short-circuiting metal transfer mode for E-1, E-2, and CSM Final are 3, 4, and 6 Hz, respectively. Calculating the actual amounts of transfer per short-circuiting event, E-1 on average transferred 0.19 grams (0.57 g/s, Table 3, divided by three short-circuiting events per second) while the CSM Final transferred 0.075 g/s (0.45 g/s, Table 3, divided by six short-circuiting events per second). The smaller mass transferred is expected to result in smoother transfer and less erratic arc behavior. In summary, the CSM Final displayed the lowest overall average voltage and also the highest and most consistent short-circuiting metal transfer mode throughout the entire weld.

Conclusions

The major conclusions of this research follow:

- A design methodology for developing SMAW consumable electrode flux coatings for high-nickel alloys is presented focusing on enhancing extrudability, weld cleanliness, slag detachability, alloying recovery, welding characteristics, and arc quality.
- A GTAW wire can be converted into a SMAW consumable electrode, thereby proving that a unified welding wire is viable for both flux coated and bare wire welding processes.
- In enhancing extrudability, an appropriate amount of binder with respect to relative humidity is important, adequate slipping agent, and a dry mix with a normal particle size distribution at 200 mesh is desirable.
- Adequate amount of cryolite is necessary for enhanced weld cleanliness for high-nickel SMAW consumable electrodes and maintaining slag viscosity. The amount must be optimized for weld cleanliness without affecting the viscosity of the slag flow since fluorides act as network breakers and decrease the viscosity of the slag.
- The CTE values for the slag and the weld metal is important for good slag detachability. Perovskite, with a CTE value of 15.8×10^{-6}/°C, had a larger CTE value than the weld metal (CTE value of 10.4×10^{-6}/°C) which exhibited the most desirable slag detachability. With a CTE value of 6×10^{-6}/°C, Sphene, a dominant slag phase, displayed poor slag detachability.
- A series of mass balance equations is presented to calculate accurate recovery rates for alloying in the flux coating developed in this research.
- Flux alloying recovery rate for chromium in this high-nickel alloy weld system was determined as 95% same as for low-carbon steel SMAW consumable electrodes.
- Manganese was calculated as 60% flux alloying recovery for this high-nickel alloy weld system which is much lower than the 75% reported in the *ASM Handbook*.
- Electrode formulation "CSM Final" exhibited the best arc stability with the lowest average voltage at 22.5 V and the lowest mass per transfer event at 0.075 g per droplet. Flux formulation is a complex, interwoven, balancing process to ensure good extrudability, welding characteristics, and weld integrity.

Acknowledgments

The authors acknowledge the help and discussions of Joe Scott and Keith Moline of Devasco International, Inc., and Bob Hamilton of Johns Manville during the course of this research. The authors also acknowledge the support of Dr. George Young for the useful discussions.

References

1. Jackson, C. E. 1973. *Fluxes and Slags in Welding*. Weld Res. Bull. 1973, No. 190, Welding Research Council, New York, N.Y.

2. Linnert, G. E. 1965. *Welding Metallurgy*. Vol. 1, Ch. 8, American Welding Society, Miami, Fla., pp. 367–396.

3. Natalie, C. A., and Olson, D. L. 1985. *Physical and Chemical Behavior of Welding Fluxes*. Center for Welding Research, Colorado School of Mines, Golden, Colo.

4. Liu, S., Frederickson, G. L., Johnson, M. Q., and Edwards, G. R. 1994. *Shielded Metal Arc Welding Consumables for Advanced High Strength Steels (HSLA-130 Steel Welding Consumables)*. Center for Welding and Joining Research, Colorado School of Mines.

5. *ASM Handbook*. Welding, Brazing, and Soldering. 1993, Vol. 6, ASM International, Materials Park, Ohio.

6. Vornovitskii, I. N., Medvedev, A. Z., and Cherkasskii, A. L. 1973. Influence of coefficient of thermal expansion of slag on its detachability from weld metal. *Svarochn. Proizvodstvo* 3: 35–37.

7. Vornovitskii, I. N., Malashonok, V. A., and Cherkasskii, A. I. 1975. Procedure for quantitative evaluation of slag detachability. *Svarochn. Proizvodstvo* 2: 47–48.

8. Olson, D. L., Liu, S., and Fleming, D. A. 1993. *Welding Flux: Nature and Behavior.* Center for Welding and Joining Research, Colorado School of Mines.

9. Donchenko, E. A., Panasenko, L. K., and Larochkin, V. K. 1978. Some properties of welding slag. *Svar. Proiz.* 6: 38–40.

10. Claussen, G. E. 1949. The metallurgy of covered electrode weld metal. *Welding Journal* 28: 12–24.

11. Scott, J., and Moline, K. 2008. Devasco International, Inc., private communication.

12. Liu, S., Dallam, C. B., and Olson, D. L. 1982. Performance of the CaF_2-CaO-SiO_2 system as a submerged arc welding flux for a niobium based HSLA steel. *Proc. Intl. Conf. on Welding Technology for Energy Applications*, Gatlinburg, Tenn., AWS-ORNL, ASM, p. 445.

13. Indacochea, J. E., and Olson, D. L. 1983. Relationship of weld metal microstructure and penetration to weld metal oxygen content. *Journal of Materials of Energy System* 5: 139.

14. Perez Guerrero, F. 2003. Effect of nickel additions of rutile electrodes for underwater welding. MS thesis, Colorado School of Mines.

15. Devries, R. C., Roy, R., and Osborn, E. F. 1955. *Phase Equilibria in the System CaO-TiO_2-SiO_2*. American Ceramic Society 38(5): 161.

16. Wu, C., et al. 2009. Plasma-sprayed $CaTiSiO_5$ ceramic coating on Ti-6Al-4V with excellent bonding strength, stability, and cellular bioactivity. *J. R. Soc. Interface* 6(31): 159–168.

17. Redfern, S. A. 1996. High-temperature structural phase transitions in perovskite ($CaTiO_3$). *J. Phys.: Condensed Matter* 8: 8267–8275.

18. Special Metals. 2008. *Inconel® 600 Alloy: Technical Bulletin*.

19. Natalie, C. A., and Olson, D. L. 1985. *Physical and Chemical Behavior of Welding Fluxes*. Center for Welding Research, Colorado School of Mines, Golden, Colo.